

## Production of Ultra-Cold-Neutrons in Solid $\alpha$ -Oxygen.

E. Gutmiedl\*,<sup>1</sup> F. Böhle,<sup>1</sup> A. Frei,<sup>1</sup> A. Maier,<sup>1</sup> S. Paul,<sup>1</sup> H. Schober,<sup>2,3</sup> and A. Orecchini<sup>2,4</sup>

<sup>1</sup>*Technische Universität München, Physik Department,  
James Franck Str. 1, D-85747 Garching, Germany*

<sup>2</sup>*Institut Laue Langevin, 6 rue Jules Horowitz, F-38042 Grenoble Cedex 9, France*

<sup>3</sup>*Universitè Joseph Fourier, UFR de Physique, F-38042 Grenoble Cedex 9, France*

<sup>4</sup>*Dipartimento di Fisica, Universit di Perugia, I-06123 Perugia,*

*and CNR-INFN CRS-Soft c/o Universit di Roma La Sapienza, I-00185 Roma, Italy.*

(Dated: October 23, 2018)

Our recent neutron scattering measurements of phonons and magnons in solid  $\alpha$ -oxygen have led us to a new understanding of the production mechanism of ultra-cold-neutrons (UCN) in this super-thermal converter. The UCN production in solid  $\alpha$ -oxygen is dominated by the excitation of phonons. The contribution of magnons to UCN production becomes only slightly important above  $E > 10$  meV and at  $E \sim 4$  meV. Solid  $\alpha$ -oxygen is in comparison to solid deuterium less efficient in the down-scattering of thermal or cold neutrons into the UCN energy regime.

PACS numbers: 28.20.Cz, 63.20.kk

Ultra-cold-neutrons (UCN) are slow enough ( $\sim 300$  neV) to be confined [1] in traps, which can be formed by materials with a high Fermi potential or by a magnetic field (60 neV/T). They can be kept for several minutes in the confinement, and thus be investigated with high precision. UCN are elementary particles that are extremely well suited for low-energy physics experiments. These experiments are investigating fundamental problems unsolved within the framework of the Standard Model [2]. One major experiment is the search for a non-zero electric dipole moment of the neutron [3] (current upper limit  $2.9 \cdot 10^{-26}$  e·cm). Another unique experiment is the precise determination of the lifetime [4] of the free neutron. This value has an important impact on the theory of weak interaction [5].

rors, and different groups [6–9] are working on the development of strong UCN sources, based on solid deuterium ( $sD_2$ ) as a converter for down-scattering of thermal or sub-thermal neutrons into the UCN energy region. Solid oxygen could be a valuable alternative when grown in the  $\alpha$ -phase ( $\alpha$ - $sO_2$ ). Solid  $\alpha$ - $sO_2$  has a 2-dimensional anti-ferromagnetic structure [10], which exhibits in addition to phonons spin wave excitations (magnons). This supplementary magnetic scattering of neutrons considered for the first time by *Liu and Young* [11] might be a strong down-conversion channel, which would enhance the production of UCN. Different groups [12, 13] performed experiments concerning UCN production in such a converter. Their results are inconclusive and a challenge to investigate  $\alpha$ - $sO_2$  further. It seems that preparation of this cryo-solid is crucial. The exact knowledge of the inelastic scattering channels in solid  $\alpha$ - $O_2$  is therefore very important.

To this aim we have measured the phonon/magnon system in  $\alpha$ - $sO_2$  by neutron time-of-flight (TOF) measurements at the IN4 spectrometer (Institute Laue-Langevin Grenoble - ILL). Thermal neutrons with an energy of  $E_0 = 16.7$  meV were used to determine the scattering function  $S(Q, E)$  in the range from 0 – 14 meV. The experimental setup (sample cell, gas system and slow control) was the same as it was used in the measurements of the dynamical neutron scattering function of  $sD_2$  [14]. We used oxygen gas with a purity  $\geq 99.999\%$ . Our measurements were performed without any external magnetic field. The  $\alpha$ - $sO_2$  crystals were prepared from liquid via the  $\gamma$ - and  $\beta$ -phase [15]. The phase transition  $\gamma$  to  $\beta$  at  $T=43.8$  K at vapor pressure was done in our experiments very slow (10 mK/h) in order to get optical semi-transparent crystals [16].

The measured scattering function  $S_{\text{data}}(Q, E)$ , the gen-

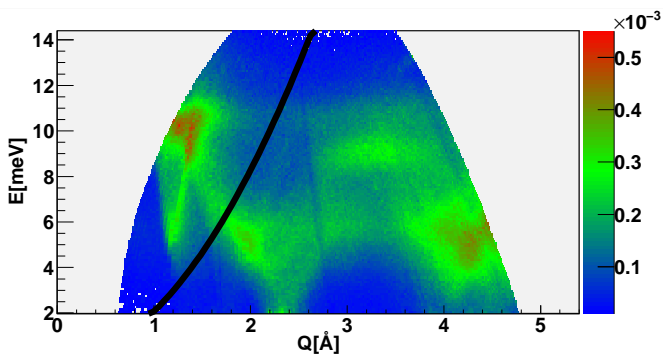


FIG. 1:

$S(Q, E)$  (arib. units) of  $\alpha$ - $sO_2$  at  $T = 5$  K. Data from IN4 measurements. Black parabola: Dispersion of the free neutron

Powerful UCN sources are needed for the experiments mentioned above in order to minimize the statistical er-

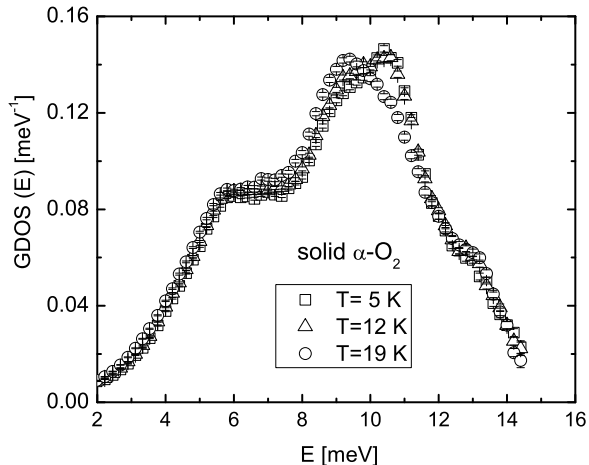


FIG. 2:

Generalized density of states  $GDOS(E)$  of  $\alpha$ -sO<sub>2</sub> at 5 K ( $\square$ )/12 K ( $\triangle$ )/19 K ( $\circ$ ). Data from IN4 measurements. GDOS is normalized to  $\int_0^\infty GDOS(E) \cdot dE = 1$

eralized density of states  $GDOS(E)$  and the cross section  $d\sigma/dE$  of  $\alpha$ -sO<sub>2</sub> are shown in Fig. 1, Fig. 2 and Fig. 3. Theoretical calculations predict [11, 17] magnetic excitations at  $E \sim 1-4$  meV. The intensities of these excitations should be primarily found at low  $Q$ -values ( $Q \ll 1 \text{ \AA}^{-1}$ ). They thus do not fall into the observation window of our experiment on the energy-loss side (see Fig. 1). However, the free neutron parabola does not cross this region and as consequence those excitations cannot contribute to the down-scattering process from the thermal into the UCN-region (see further down). The cross section  $d\sigma/dE$  (see Fig. 3) shows on the energy gain side only up-scattering close to  $E=0$  (elastic peak). This up-scattering in our data is very likely triggered by phonons. This experimental observation should induce a large mean free path ( $\lambda_{mfp}$ ) of UCN in  $\alpha$ -sO<sub>2</sub>, as it was predicted by *Liu and Young* [11]. Neutron scattering by solid oxygen is purely coherent and mostly elastic ( $\sigma_{el}/\sigma_{tot} \sim 0.84$  - value deduced from our neutron scattering data - see Fig. 3). The elastic Bragg peaks in Fig. 1 are cut out in order to enhance the contrast for the inelastic scattering in the plot. The GDOS can be calculated from  $S(Q, E)$  [18] by sampling over a large  $Q$ -range (neutron energy loss side), and applying the incoherent approximation [19]. The GDOS can be deduced by

$$GDOS(E) = E \cdot \frac{S(Q(< 2\theta >), E)}{Q^2 \cdot (n+1)}. \quad (1)$$

The term  $Q(< 2\theta >)$  is a  $Q$  value for each energy transfer  $E$  considering an averaged scattering angle  $< 2\theta >$ , while  $n$  is the Bose distribution for the phonons.

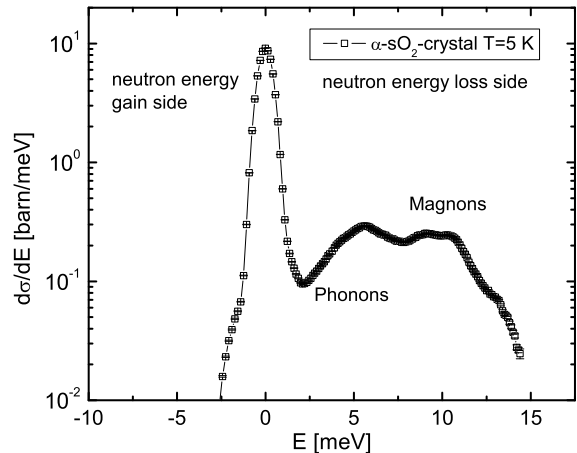


FIG. 3:

$d\sigma/dE$  of  $\alpha$ -sO<sub>2</sub> at  $T = 5$  K. Data from IN4 measurements.

Although oxygen is a purely coherent scatterer, it can be useful to use this approximation to obtain an estimate of the excitation spectra in the sample [20]. First results of the generalized density of states ( $T \simeq 4$  K and 23 K) were published by *de Bernabe et al.* [21] and *Kilburn et al.* [22]. Their results show a mixture of phonons, librins and anti-ferromagnetic excitations (magnons). The peak at  $E \simeq 10.5$  meV at  $T=5$  K in our result is more pronounced compared to the result of *de Bernabe et al.*. The GDOS at  $T=10$  K of *Kilburn et al.* is more equal to our result at  $T=5$  K. At higher temperatures our GDOS and *de Bernabe et al.* GDOS are showing similar structures. Calculated contributions of magnons (see Fig. 6 in [21]) should appear at  $E \simeq 5$  meV and  $E \simeq 12.5$  meV, which are neither detected in our or their data. The magnon peak positions at lower energies are explained by *de Bernabe et al.* by a decrease of the exchange constant (see Eq. (6) in [21]) with decreasing temperature. A more general detailed analysis of our neutron scattering data will be presented in a forthcoming paper.

These experimental findings in our data have an important impact on the UCN production in solid oxygen. The dynamical scattering function of solid oxygen resolved from our neutron scattering data has to be calibrated to absolute values. This calibration uses the known value of the total cross section for thermal neutron energies.

$$\sigma_{tot}(E_0) = \int_0^\infty dE_f \int \frac{k_f}{k_0} b_{eff}^2 S(Q, E) d\Omega. \quad (2)$$

The wave vector and the energy of the scattered neutrons in Eq. (2) are  $k_f$  and  $E_f$ , whereas  $k_0$  is the wave vector of the incident neutrons. The effective scattering length  $b_{eff}^2 = 2 \cdot b_{nucl}^2 + b_{mag}^2$  contains a combination

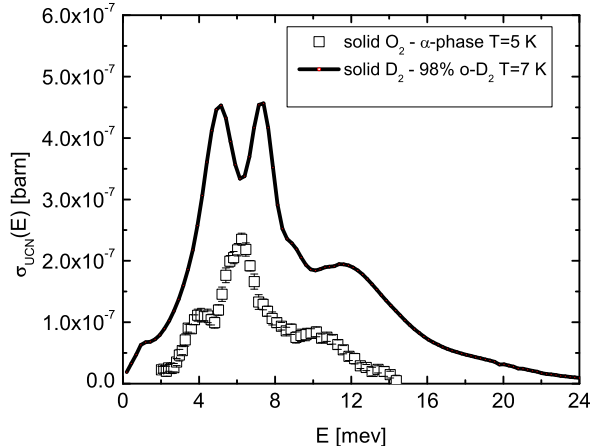


FIG. 4:

UCN production cross section of  $\alpha$ -sO<sub>2</sub> ( $\square$ ) at  $T=5$  K and sD<sub>2</sub> (98% ortho concentration) (line) at  $T=7$  K. UCN energy range 0-140 neV inside the solid D<sub>2</sub>, UCN energy range 0-163 neV inside the solid  $\alpha$ -sO<sub>2</sub>. Cross section determined by a integration of  $S(Q, E)$  along the free dispersion of the neutron. Data from IN4 measurements.

of nuclear ( $b_{\text{nuc}} = 5.8$  fm [23]) and magnetic scattering ( $b_{\text{mag}} = 5.38$  fm [11]). The dynamical scattering function can be calculated via

$$S(Q, E) = \kappa \cdot S_{\text{data}}(Q, E). \quad (3)$$

The value of the calibration factor  $\kappa = 1240$  is obtained by using Eq. (2) and the knowledge of the total cross section ( $\sigma_{\text{tot}}(E_0=16.7 \text{ meV}) \approx 4\pi b_{\text{eff}}^2 = 12.1$  barn). In the case of UCN production the following relations are valid:  $E_f = E_U \ll E_0$ ;  $E = E_0 - E_f \sim E_0$ , where  $E_0$  is the initial energy of the neutron before scattering. The UCN production cross-section can be determined by direct integration of the dynamic neutron cross section data in the kinematic region along the free neutron dispersion parabola ( $E_0 \approx \hbar^2 Q^2 / 2m$ )

$$\sigma_{\text{UCN}}(E_0) = \int_0^{E_U^{\text{max}}} \frac{d\sigma(E_U)}{dE_0} dE_U. \quad (4)$$

The evaluation of the integral (Eq. (4)) uses the dynamic scattering function  $S(Q, E = \frac{\hbar^2}{2m} k_0^2)$  at the phase space points of the neutron parabola. The UCN production cross section can, therefore be expressed by

$$\sigma_{\text{UCN}}(E_0) = \frac{\sigma_0}{k_0} S(k_0, \frac{\hbar^2}{2m} k_0^2) \frac{2}{3} k_U^{\text{max}} E_U^{\text{max}}. \quad (5)$$

The term  $E_0 = \frac{\hbar^2}{2m} k_0^2$  is the energy for an incoming neutron with wave vector  $k_0$ , whereas  $\sigma_0$  is the total cross

section ( $\sigma_0 = 4\pi b_{\text{eff}}^2$ ). The result for  $\sigma_{\text{UCN}}(E)$  is shown in Fig. 4. For comparison the UCN production cross section for ortho-sD<sub>2</sub> is also included in Fig. 4 (line).

When determining the upper limit of the integration we have to take into account that the UCN will gain kinetic energy when leaving the converter [24]. UCN produced in sD<sub>2</sub> gain  $\Delta E_U \sim 110$  neV, while the energy gain for  $\alpha$ -sO<sub>2</sub> is  $\Delta E_U \sim 87$  neV. Therefore, the upper limit of the energy the neutrons are allowed to have inside the converters was set to  $E_U^{\text{max}}(\alpha\text{-sO}_2) = 163$  neV and  $E_U^{\text{max}}(\text{ortho-sD}_2) = 140$  neV. These limits correspond to an upper limit of  $E_U^{\text{max}} = 250$  neV outside the converter (Fermi potential of UCN guide). The calculation of UCN production cross section of sD<sub>2</sub> was performed using the incoherent approximation [19] and recently published data [14] for the density of states in sD<sub>2</sub>.

In  $\alpha$ -sO<sub>2</sub> the parabola of the free neutron crosses in the scattering function a band of dispersive excitations at  $E \sim 6$  meV (see Fig. 1). At this point the UCN production cross section is determined by coherent phonon scattering. Therefore a major peak (Fig. 4) at  $E \sim 6$  meV can be identified with excitation of phonons (see also [17]). The structures in the UCN production cross section at  $E \sim 4$  meV and  $E \sim 10$  meV are very likely induced by magnetic scattering (magnons) [21]. The contribution of magnons at  $E \sim 4$  meV and 10-12 meV to the UCN production cross section is small compared to the phonon contribution at  $E \sim 6$  meV. Our data clearly lead to the conclusion that the creation of phonons is the main energy loss channel in the conversion process of  $\alpha$ -sO<sub>2</sub>. In comparison to solid ortho-deuterium (see Fig. 4)  $\alpha$ -sO<sub>2</sub> possesses a remarkably poorer capacity of creating UCN by down-scattering of thermal and sub-thermal neutrons. This result can be explained by a larger inelastic cross section of ortho-sD<sub>2</sub> ( $T \simeq 7$  K) compared to  $\alpha$ -sO<sub>2</sub> at thermal neutron energies [25]. The ratio of the two inelastic cross sections is  $\sigma_{\text{inel}}(\text{ortho-sD}_2) / \sigma_{\text{inel}}(\alpha\text{-sO}_2) \simeq 4.7$  at  $E_0 = 16.7$  meV. On the other hand  $\alpha$ -sO<sub>2</sub> should exhibit a large mean free path for UCN inside the converter as it is predicted by *Liu and Young* [11] and also indicated by our data (see Fig. 3). Values up to  $\lambda_{\text{mfp}} \simeq 4$  m are expected. This opens the opportunity to construct a large UCN source with this material. This kind of large source could defeat a sD<sub>2</sub> source due to the small mean free path (several cm [6]) of UCN in solid deuterium. We recently have measured directly the UCN production in  $\alpha$ -sO<sub>2</sub> [26]. From our data we could extract a  $\lambda_{\text{mfp}} \simeq 0.3$  m at  $T \simeq 8$  K. This mean free path increases to  $\lambda_{\text{mfp}} \simeq 3$  m at  $T \simeq 5$  K and confirms the predictions made by *Liu and Young* [11]. Furthermore we could deduce an average final energy of  $E_f \sim 3$  meV after up-scattering of UCN from our new data [26]. This value for the final energy could be provided by the predicted magnon excitations. At 5 K the occupation of such modes is such that the corresponding intensities become unobservable in our scattering experiment, while it is still

sufficient to provide observable upscattering of UCN.

The UCN production rate  $P_{UCN}$  [UCN/cm<sup>3</sup> s] of  $\alpha$ -sO<sub>2</sub>, which is exposed to a neutron spectrum  $d\Phi/dE$  with maxwellian energy distribution ( $T_n$  - Effective temperature of the incoming neutron spectrum) can be calculated by

$$P_{UCN}(T_n) = N_{O_2} \cdot \int_0^{E_{max}} \frac{d\Phi(T_n)}{dE_0} dE_0 \cdot \sigma_{UCN}(E_0). \quad (6)$$

$N_{O_2} = 2.9 \cdot 10^{22} \text{ cm}^{-3}$  is the particle density of the O<sub>2</sub> molecules. Fig. 5 shows the result for  $P_{UCN}(T_n)$  for sD<sub>2</sub> and sO<sub>2</sub>. Contrary to the results published in [11] (optimal  $T_n \approx 10 - 15 \text{ K}$ ) the UCN production rate has a maximum at  $T_n \approx 40 \text{ K}$ .

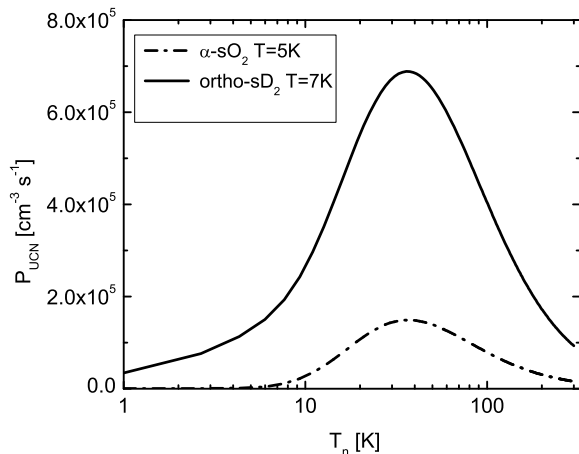


FIG. 5:

Calculated UCN production rate of ortho-sD<sub>2</sub> at  $T = 7 \text{ K}$  (line) and  $\alpha$ -sO<sub>2</sub> at  $T = 5 \text{ K}$  (dash-dot line). Both converters are exposed to a neutron capture flux of  $\Phi_C = 1 \cdot 10^{14} \text{ cm}^{-2} \text{ s}^{-1}$  (Maxwellian shape with effective temperature  $T_n$ ).

In summary, new neutron scattering data of solid  $\alpha$ -oxygen leads to a better understanding of UCN production in this converter material. The new results for the UCN production cross section, resolved directly from the dynamical scattering function  $S(Q, E)$ , show a significant UCN production cross section for neutrons with energies at  $E_0 \sim 6 \text{ meV}$ . The leading excitations are phonons and not magnons. This observation is different to predictions of theoretical calculations [11] where the authors predict the contributions of magnons to the UCN production, and identified these excitations as the leading process of UCN production in solid  $\alpha$ -oxygen. An optimized  $\alpha$ -sO<sub>2</sub> UCN source should be exposed to a cold neutron flux with an effective neutron temperature of  $T_n \simeq 40 \text{ K}$ , where the production rate has a maximum. At this tem-

perature the UCN production rate of  $\alpha$ -sO<sub>2</sub> is only 22 % of the production rate of sD<sub>2</sub>.

This work was supported by the cluster of excellence "Origin and Structure of the Universe" (Exc 153) and by the Maier-Leibnitz-Laboratorium (MLL) of the Ludwig-Maximilians-Universität (LMU) and the Technische Universität München (TUM). We thank T. Deuschle, S. Materne, C. Morkel, and H. Ruhland for their help during the experiments.

- 
- [1] R. Golub, D. Richardson, S.K. Lamoreaux, Ultra-Cold Neutrons, Adam Hilger, Bristol, Philadelphia and New York (1991).
  - [2] M.J. Ramsey-Musolf, Nucl. Instrum. Methods Phys. Res. **A 611**, 111 (2009).
  - [3] C.A. Baker et al., Phys. Rev. Lett. **97**, 131801 (2006).
  - [4] S. Paul, Nucl. Instrum. Methods Phys. Res. **A 611**, 157 (2009).
  - [5] K. Schreckenbach, J. Phys. G. **14**, S391 (1988).
  - [6] A. Frei et al., EPJ **A 34**, 119 (2007).
  - [7] Roger E. Hill et al., Nucl. Instrum. Methods Phys. Res. **A 440**, 674 (2000).
  - [8] A. Anghel et al., Nucl. Instrum. Methods Phys. Res. **A 611**, 272 (2009).
  - [9] A. Serebrov et al., JETP Lett. **62**, 785 (1995).
  - [10] P.W. Stephens and C.F. Majkrzak, Phys. Rev. B **33**, 1 (1986).
  - [11] C.-Y. Liu and A.R. Young, arXiv:nucl-th/0406004v1, (2004).
  - [12] Malgorzata Kasprzak, Ultracold Neutron converters, Di-ssertation, University of Vienna (2008), [http://ucn.web.psi.ch/papers/MKasprzak\\_thesis2008.pdf](http://ucn.web.psi.ch/papers/MKasprzak_thesis2008.pdf).
  - [13] D. Salvat et al., 7th International UCN Workshop, St. Petersburg, Russia (2009), <http://cns.pnpi.spb.ru/ucn/index.html>.
  - [14] A. Frei et al., Phys. Rev. B. **80**, 064301 (2009).
  - [15] Yu.A. Freiman and H.J. Jodl, Physics Reports **401**, 1-228 (2004).
  - [16] Ralitsa Bozhanova Bozhanova, Optical investigations of solid oxygen in the  $\alpha$ -phase, Bachelor Thesis, Technical University of Munich (2009), <http://www.e18.physik.tu-muenchen.de/>.
  - [17] A.P. Jansen and A. van der Avoird, J. Chem. Phys. **86**, 3583 (1987).
  - [18] G.L. Squires, Introduction to the theory of thermal neutron scattering, Cambridge, New York: Cambridge University Press, (1978).
  - [19] V.F. Turchin, Slow Neutrons, Israel Program for Scientific Translations, Jerusalem, (1965).
  - [20] N. Breuer, Z. Physik **271**, 289 (1974).
  - [21] A. de Bernabe, G.J. Cuello, F.J. Bermejo, F.R. Trouw, A.P.J. Jansen, Phys. Rev. B **58**, 14442 (1998).
  - [22] D. Kilburn, P.E. Sokol, C.M. Brown, Phys. Rev. B **78**, 214304-1 (2008).
  - [23] <http://ftp.ncnr.nist.gov/resources/n-lengths/>.
  - [24] I. Altarev et al., Phys. Rev. Lett. **100**, 014801 (2008).
  - [25] F. Atchison et al., Nucl. Instrum. Methods Phys. Res. **A 611**, 252 (2009).
  - [26] A. Frei et al., arXiv:nucl-ex/1006.2970v1, (2010).